Nonadditive Voltammetric Currents from Two Redox-Active Substances and Electroanalytical Implications

ARTICLE *in* ANALYTICAL CHEMISTRY · SEPTEMBER 2003

Impact Factor: 5.64 · DOI: 10.1021/ac030176u

4 AUTHORS, INCLUDING:

Woon su Oh
LG Innotek R&D CENTER
11 PUBLICATIONS **165** CITATIONS
SEE PROFILE

Abdel Monem Rawashdeh
Missouri University of Science and Technology
40 PUBLICATIONS **622** CITATIONS
SEE PROFILE

Anal. Chem. **2003,** *75,* 4996−5005

Nonadditive Voltammetric Currents from Two Redox-Active Substances and Electroanalytical Implications

Nicholas Leventis,* Woon Su Oh, Xuerong Gao, and Abdel-Monem M. Rawashdeh

Department of Chemistry, University of Missouri−Rolla, Rolla, Missouri 65409

At the potential range where both decamethylferrocene (dMeFc) and ferrocene (Fc) are oxidized with rates controlled by linear diffusion, electrogenerated $Fc^{\bullet+}$ radicals diffusing outward from the electrode react quantitatively ($K_{23^\circ C} = 5.8 \times 10^8$) with dMeFc diffusing toward the electrode and produce Fc and $dMeFc^{\bullet+}$. That reaction replaces dMeFc with Fc, whose diffusion coefficient is higher than that of dMeFc, and the total mass-transfer limited current from the mixture is increased by ∼10%. Analogous observations are made when mass transfer is controlled by convective diffusion as in RDE voltammetry. Similar results have been obtained with another, and for all practical purposes randomly selected pair of redox-active substances, $[Co(bipy)_3]^{2+}$ and *N*-methylphenothiazine (MePTZ); reaction of $MePTZ^{\bullet+}$ with $[Co(bipy)_3]^{2+}$ replaces the latter with MePTZ, which diffuses faster, and the total current increases by ∼20%. The experimental voltammograms have been simulated numerically and the role of (a) the rate constant of the homogeneous reaction, (b) the relative concentrations, and (c) the diffusion coefficients of all species involved have been studied in detail. Importantly, it was also identified that within any given redox system the dependence of the mass-transfer limited current on the bulk concentrations of the redox-active species is expected to be nonlinear. These findings are discussed in terms of their electroanalytical implications.

Voltammetry is the recording of the electric current, *i*, flowing through an electrolytic solution as a function of the applied potential, *E*.[1] Voltammetric methods such as dropping mercury electrode polarography, cyclic voltammetry (CV), sampled current voltammetry (SCV), normal pulse voltammetry (NPV), differential pulse voltammetry (DPV), rotating disk electrode (RDE) voltammetry, and several others may differ either in the electrode configuration or the waveform of *E*, but all produce *i*−*E* curves, whose position in the *E* direction is related to the formal potentials ($E^{\circ\prime}$) of the redox-active species and their size in the *i* direction is related to the concentration of the redox-active species.

These concepts have been particularly useful in the analysis of mixtures of redox-active species. For example, a solution containing two redox-active species R_1 and R_2, which can be oxidized to redox forms O_1 and O_2, respectively (eqs 1 and 2),

$$R_1 - e \rightleftarrows O_1 \quad (1)$$

$$R_2 - e \rightleftarrows O_2 \quad (2)$$

produces two distinct "waves", centered around the $E^{\circ\prime}$ values of the two couples, O_1/R_1 and O_2/R_2. Now, let $E^{\circ\prime}_{O_2/R_2} > E^{\circ\prime}_{O_1/R_1}$, so R_1 undergoes oxidation to O_1 (eq 1) before R_2 undergoes oxidation to O_2 (eq 2). Using, for example, SCV or NPV one obtains a double sigmoid *i*−*E* curve with two current plateaus. The first plateau is due to eq 1 and the second one to eqs 1 and 2 taking place concurrently with diffusion-controlled rates. The standard practice has been to consider the currents allocated to eqs 1 and 2 as additive.[1,2] Therefore, if diffusion is linear, in both methods the limiting current, i_d, at the second plateau is given by eq 3, where

$$i_d = (FA/\pi^{1/2}\tau^{1/2})(D_{R_1}^{1/2} C_{R_1}^* + D_{R_2}^{1/2} C_{R_2}^*) \quad (3)$$

F is the Faraday constant, *A* is the electrode area, τ the time at which the chronoamperometric current is sampled, and D_{R_1}, D_{R_2}, and $C_{R_1}^*$ are the diffusion coefficients and the bulk concentrations of species R_1 and R_2, respectively.[1,2] Consequently, subtracting from i_d the current allocated to the oxidation of R_1 ($i_{l,R_1} = FA D_{R_1}^{1/2} C_{R_1}^*/\pi^{1/2}\tau^{1/2}$) allows calculation of the current allocated to the oxidation of R_2 (i_{l,R_2}). Then, if either the diffusion coefficient D_{R_2} or a relative response factor between R_1 and R_2 is known, the concentration of R_2 is calculated readily. But is this so?

Despite the fact that a great deal of quantitative analysis is based on that methodology, it is shown here that in general eq 3 is experimentally invalid, and therefore, its use may lead to substantial error. For this, we employ two pairs of redox-active substances: decamethylferrocene/ferrocene (dMeFc/Fc) and

* Corresponding author. Current address: Materials Division, NASA Glenn Research Center, 21000 Brookpark Rd., M.S. 49-1, Cleveland, OH 44135. Tel.: (216) 433-3202. E-mail: Nicholas.Leventis@grc.nasa.gov.

(1) (a) Bard, A. J.; Faulkner, L. J. *Electrochemical Methods, Fundamentals and Applications*, 2nd ed.; Wiley: New York, 2000. (b) Bard, A. J.; Faulkner, L. J. *Electrochemical Methods, Fundamentals and Applications*; Wiley: New York, 1980.

(2) See, for example: (a) Skoog, D. A.; Holler, F. J.; Nieman, T. A. *Principles of Instrumental Analysis*, 5th ed.; Saunders College Publishing: Philadelphia, PA, 1998; p 649. (b) Willard, H. H.; Merritt, L. L., Jr.; Dean, J. A.; Settle, F. A., Jr. *Instrumental Methods of Analysis*, 6th ed.; Wadsworth Publishing Co.: Belmont, CA, 1981; p 720.

10.1021/ac030176u CCC: $25.00
Published on Web 09/03/2003

$[Co(bipy)_3]^{2+}$/*N*-methylphenothiazine (MePTZ) (bipy = 2,2′-bipyridine.) The first pair was selected because ferrocene is a widely accepted internal standard. The second pair represents two random redox-active substances that may be encountered in solution. In both cases, the deviation of the mass-transfer limited current at the second plateau from what is expected by simple superposition of the currents obtained from each member of the pair separately is significant. For about equal concentrations, in the former pair, the second wave (corresponding to the oxidation of ferrocene) is larger than what is expected via eq 3 by ~10%, while in the latter case, the second wave (corresponding to the oxidation of *N*-methylphenothiazine) is larger by ~20%. These phenomena are quite general and have been observed not only with SCV and NPV but also with CV, RDE voltammetry, and DPV. In that regard, what is particularly disturbing is that depending on the analyte DPV can be a more sensitive analytical method even than molecular or atomic absorption spectroscopy;[1] clearly, however, if its reliability is compromised, its sensitivity becomes irrelevant. Furthermore, the results with ferrocene point out that even the routine use of that compound as a general-purpose internal redox-potential standard should also be questioned: it was found that since the current from the oxidation of Fc is resized, its half-wave potential ($E_{1/2}$) is also repositioned.

These phenomena are traced to the fact that electrogenerated O_2 diffusing away from the electrode, reacts with R_1 diffusing toward the electrode (eq 4). The driving force of eq 4 depends

$$O_2 + R_1 \overset{K}{\rightleftharpoons} R_2 + O_1 \qquad (4)$$

on the difference $\Delta E°$ between the two standard potentials ($E°_{O_2/R_2}$ and $E°_{O_1/R_1}$) and can be large. If, for example, $\Delta E° \approx 0.515$ V (as in the case of the dMeFc/Fc pair), the equilibrium constant $K_{23°C}$ of eq 4 at 23 °C is $\sim 5.8 \times 10^8$; if $\Delta E° \approx 0.418$V (as in the case of the $[Co(bipy)_3]^{2+}$/MePTZ pair), $K_{23°C} \approx 1.3 \times 10^7$. The effect of eq 4 is to replace, at least partially, R_1 with R_2, which also diffuses toward the electrode. Unless $D_{R_1} = D_{R_2}$, the additional flux of R_2 does not counterbalance the lost flux of R_1, and the mass-transfer limited current at sufficient positive potentials is not equal to what is calculated via eq 3. This situation is analogous to that observed at the second current plateau in the presence of a homogeneous comproportionation reaction between any redox-active species R, and its two-electron (2-e) oxidized (or reduced) form, O_2 (eq 5).[3−5] That reaction yields 2 equiv of the intermediate

$$R + O_2 \rightleftharpoons 2O_1 \qquad (5)$$

1-e redox state, O_1, and again unless $D_R = D_{O_1}$, the limiting current from the 2-e oxidation or reduction of R is not twice the current from the 1-e process.[3,5] Despite the similarity of eqs 4 and 5, the practical consequences of the latter are not severe, because at worse it may lead to a miscalculation of D_R. However, in the case of a mixture of redox-active substances, eq 4 may lead to miscalculation of a concentration in situations where there may be no means for independent validation.

The voltammetric effect of certain nonredox-type homogeneous reactions following the second electron transfer has been considered even from the early stages of the development of polarography as an electroanalytical method. In those early examples, the second limiting current was greatly diminished as R_1 could not reach the electrode, not because of being replaced by R_2 (eq 4), but because of a precipitation-type reaction with a product of the second redox process.[6,7] Meanwhile, homogeneous reactions of eq 4-type have become very common: they are introduced deliberately in order to carry out mediated oxidation (or reduction) of a species R_1 by electrogenerated redox-form O_2;[8] they are encountered at a liquid/liquid interface near the ultramicroelectrode (UME) tip of a scanning electrochemical probe,[9] and they maintain steady-state conditions in certain two-electrode thin-layer cells operating as solution-phase electrochromic devices.[10] The effect of $D_{R_1} \neq D_{R_2}$ on the total chronoamperometric current when all four species of eq 4 remain in solution was first considered by Andrieux et al.[11] Interestingly, upon detailed analysis of eq 4, those authors were also able to identify an analytical expression for the total chronoamperometric current in the rather uncommon case where the equilibrium constant $K = 1$ (i.e., for overlapping waves);[11] Anson extended the analysis of that special case and showed equivalence between chronoamperometry and RDE voltammetry (i.e., a diffusion-controlled method and a convective diffusion-controlled method).[12] As it will become apparent from the ensuing discussion, although those earlier studies are fundamental in describing the phenomena associated with eq 4, nevertheless they offer little practical utility from an electroanalytical point of view. The goal of this paper is to bridge that gap and furnishes the first experimental comparison (involving practically all of the main voltammetric methods) of what the total voltammetric current from two redox-active species should have been if faradaic currents were additive versus what actually is. The results are confirmed theoretically via digital simulations and the role of all controlling parameters, namely, rate constants, relative concentrations and diffusion coefficients have been investigated in detail. Furthermore, to our knowledge this is also the first report on the role of homogeneous reactions of the eq 4-type upon half-wave potentials. Our results are discussed in terms of their electroanalytical implications, and we propose specific methodology for conducting quantitative and qualitative voltammetry and data analysis.

(3) Rongfeng, Z.; Evans, D. H. *J. Electroanal. Chem.* **1995**, *385*, 201.
(4) Amatore, C.; Bonhomme, F.; Bruneel, J.-L.; Servant, L.; Thouin, L. J. *Electoanal. Chem.* **2000**, *484*, 1.
(5) Leventis, N.; Gao, X. *J. Electroanal. Chem.* **2001**, *500*, 78.
(6) (a) Kolthoff, I. M.; Lingane, J. J. *Polarography*, 2nd ed.; Wiley-Interscience: New York, 1952; Vol. 1, Chapter VI. (b) Lingane, J. J. Ph.D. Thesis, University of Minnesota, 1938.
(7) It should be noted that ref 1a (p 205) does recognize that diffusion currents may not be additive and cites Lingane's precipitation example.[6]
(8) (a) Andrieux, C. P.; Hapiot, P.; Saveant, J. M. *J. Electroanal. Chem.* **1985**, *189*, 121. (b) Andrieux, C. P.; Hapiot, P.; Saveant, J.-M. *Chem. Rev.* **1990**, *90*, 723.
(9) Barker, A. L.; Unwin, P. R.; Amemiya, S.; Zhou, J.; Bard, A. J. *J. Phys. Chem. B* **1999**, *103*, 7260.
(10) (a) Leventis, N.; Chen, M.; Liapis, A. I.; Johnson, J. W.; Jain, A. *J. Electrochem. Soc.* **1998**, *145*, L55. (b) Byker, H. J. In *Electrochromic Materials II*; Ho, K. C., MacArthur, D. A., Eds.; The Electrochemical Society Proceedings Series PV 94-2; Electrochemical Society: Pennington, NJ, 1994; , p 3.
(11) (a) Andrieux, C. P.; Hapiot, P.; Saveant, J. M. *J. Electroanal. Chem.* **1984**, *172*, 49. (b) Andrieux, C. P.; Hapiot, P.; Saveant, J. M. *J. Electroanal. Chem.* **1985**, *186*, 237.
(12) Blauch, D. N.; Anson, F. C. *J. Electroanal. Chem.* **1991**, *309*, 313.

EXPERIMENTAL SECTION

Materials. dMeFc, Fc, and MePTZ were purchased from Aldrich at the highest purity available. dMeFc was used as received. Fc and MePTZ were purified further by sublimation. $[Co(bipy)_3](ClO_4)_2$ was available from prior work.[13] $[Co(bipy)_3](ClO_4)_3 \cdot 3H_2O$ was synthesized from $CoCl_2$ according to the literature: ^{1}H NMR (CD_3CN, 400 MHz) δ 7.29 (6H, dd, $J_1 = 6.0$ Hz, $J_2 = 0.8$ Hz), 7.72−7.76 (6H, m), 8.45−8.49 (6H, m), 8.70 (6H, dd, $J_1 = 8.4$ Hz, $J_2 = 1.2$ Hz). Anal. Calcd for $CoC_{30}H_{30}N_6O_{15}Cl_3$: C, 40.95; H, 3.44; N, 9.55. Found: C, 40.99; H, 3.16; N, 9.52.[14]

Anhydrous CH_3CN was purchased from Aldrich. $LiClO_4$ (Aldrich) was dried under vacuum. Tetrabutylammonium perchlorate (TBAP) was prepared from an aqueous solution of tetrabutylammonium bromide (Aldrich) and 70% aqueous $HClO_4$ as described before.[5]

Equipment. All electrochemical experimentation was conducted with either a EG&G 263A or a EG&G 283 potentiostat controlled by the EG&G model 270/250 Research Electrochemistry Software 4.30. For rotating electrode experiments, we used a AFMSRX rotator (Pine Instrument Co.). Gold disk working electrodes (1.6-mm diameter, 0.0201 cm^2) and Ag/AgCl/aqueous KCl (3 M) reference electrodes were purchased from Bioanalytical Systems, Inc. For the RDE experiments, we employed a Au−Au ring−disk electrode system (disk diameter, 2.29 mm; inner ring diameter, 2.46 mm; outer ring diameter, 2.69 mm) purchased from Pine Instruments Co. As a counter electrode we used a gold foil (2.5 cm^2 on each side).

Methods. All volumetric ware was rinsed with acetone, washed with Micro cleaning solution in boiling water, rinsed with copious amounts of water, and dried at 150 °C. The counter electrode was cleaned in a 1:4 (v/v) H_2O_2/c H_2SO_4 solution, rinsed with water, and oven-dried. The working electrode was polished successively with 6-, 3-, and 1-μm diamond paste, washed with water and acetone, and air-dried.

Solutions of dMeFc, Fc, $[Co(bipy)_3]^{2+}$, and MePTZ (~3 mM) were first characterized voltammetrically and subsequently equal volumes (5.00 mL) of (a) the dMeFc and Fc or (b) the $[Co(bipy)_3]^{2+}$ and MePTZ solutions were mixed and characterized again. All electrochemical experimentation was conducted at room temperature (23 ± 1 °C), with 80% compensation for the solution resistance.

Ratios between the diffusion coefficients of dMeFc, Fc, and MePTZ and their oxidized forms $dMeFc^{\bullet+}$, $Fc^{\bullet+}$, and $MePTZ^{\bullet+}$ respectively, were determined by a combination of bulk electrolysis/UME voltammetry as we have described in more detail before.[5] In a typical procedure, a solution of, for example, Fc was characterized first with the UME before electrolysis. Subsequently, electrolysis was conducted until the current declined to ~0.5% of its original value (~5 min), and the resulting solution of $Fc^{\bullet+}$ was characterized with the UME. The $D_{Fc}/D_{Fc^{\bullet+}}$ ratio is equal to the ratio of the UME mass-transfer limited currents before and after electrolysis. Finally, a second bulk electrolysis converted $Fc^{\bullet+}$ back to Fc and the solution was characterized with the UME one last time in order to determine the percent recovery of Fc, which is an indication of the stability of the radical and therefore of the reliability of the data. In all cases, the recovery was 100 ± 2%.

(13) Leventis, N.; Gao, X. *J. Am. Chem. Soc.* **2002**, *124*, 1079.
(14) Burstall, F. H.; Nyholm, R. S. *J. Chem. Soc.* **1952**, 3570.

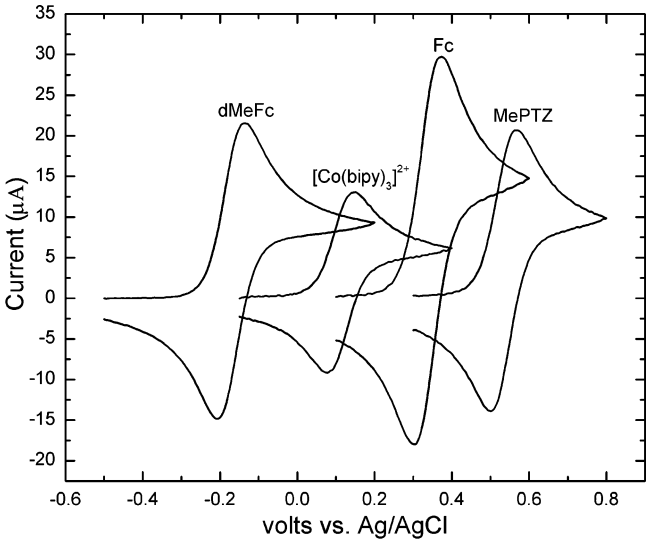

Figure 1. Cyclic voltammetric characterization of separate solutions, each containing one of the four redox-active species used in this study: dMeFc (3.22 mM) and Fc (3.23 mM) in CH_3CN/0.1 M TBAP. $[Co(bipy)_3]^{2+}$ (3.06 mM) and MePTZ (3.04 mM) in CH_3CN/1.0 M $LiClO_4$. Using a Au disk electrode (0.0201 cm^2) swept at 0.1 V s^{-1}.

(The occasionally slightly higher than 100% recovery was attributed to loss of a small amount of solvent by evaporation, due to the continuous bubbling of Ar and vigorous stirring of the solution throughout the experiment.)

Digital simulations were carried out on an iMac G3 Macintosh computer using an Absoft Corporation Fortran 77 Compiler 4.4.[5]

RESULTS

A general electrochemical characterization of the four compounds used in this study is shown in Figure 1. The voltammograms were obtained in separate solutions of about equal concentrations in dMeFc, Fc, $[Co(bipy)_3]^{2+}$, and MePTZ. The quite different size of the four voltammograms is due primarily to the different diffusion coefficients of the four compounds (Table 1) and secondarily to the small differences in concentration. Since knowledge of diffusion coefficients in our electrolytic systems is of pivotal importance for this work, $D_{Fc,}$ D_{dMeFc}, and D_{MePTZ} were determined from the chronoamperometric data generated in this study. $D_{Co(II)}$ was derived from two different series of chronoamperometric experiments where the concentration of $[Co(bipy)_3]^{2+}$ was varied from 3 to 100 mM. (The correlation of the Cottrell slope vs concentration was 0.998 and 0.999 for each experiment, respectively.) With the exception of $[Co(bipy)_3]^{2+}$, the ratio of the diffusion coefficients of each compound and its oxidized form, D_R/D_O, was obtained by a combination of bulk electrolysis and UME voltammetry as described in the Experimental Section. The diffusion coefficient ratio $D_{Co(II)}/D_{Co(III)}$ was calculated from the actual diffusion coefficients of the two redox forms.

For our purposes, the four compounds above are considered in pairs, and the effect of eq 4 on linear diffusion-controlled electrochemical methods is demonstrated with NPV, SCV, CV, and DPV using conventional disk millielectrodes. The effect of eq 4 on convective diffusion-controlled methods is demonstrated with RDE voltammetry.

Decamethylferrocene/Ferrocene System. Figure 2A shows representative NPVs of two separate solutions, one containing

Table 1. Diffusion Coefficient Data for the Four Compounds of This Study (in $cm^2\ s^{-1}$)

D_{dMeFc}[a]	D_{Fc}[a]	$D_{Co(II)}$[b]	D_{MePTZ}[b]
$(1.9 \pm 0.1) \times 10^{-5}$ (25)[c]	$(3.2 \pm 0.2) \times 10^{-5}$ (22)[c]	$(6.0 \pm 0.3) \times 10^{-6}$ [d]	$(1.7 \pm 0.1) \times 10^{-5}$ (7)[c]
$D_{dMeFc}/D_{dMeFc^{\bullet+}}$	$D_{Fc}/D_{Fc^{\bullet+}}$	$D_{Co(II)}/D_{Co(III)}$	$D_{MePTZ}/D_{MePTZ^{\bullet+}}$
1.04 ± 0.01[e]	1.05 ± 0.02[e]	1.02[f]	1.22 ± 0.01[e]

[a] In CH_3CN/0.1 M TBAP. [b] In CH_3CN/1.0 M $LiClO_4$. [c] In parentheses is the number of independent experimental results used for averaging. For the 95% confidence limit multiply the standard deviations by a factor of 2. [d] The error is the spread of the diffusion coefficients derived from two different series of chronoamperometric experiments (see text). [e] By bulk electrolysis/UME voltammetry (see Experimental Section). [f] By dividing $D_{Co(II)}$ by $D_{Co(III)}$; $D_{Co(III)} = (5.9 \pm 0.8) \times 10^{-6}$ $cm^2\ s^{-1}$ (average of nine chronoamperometric experiments in the range 1−5 mM).

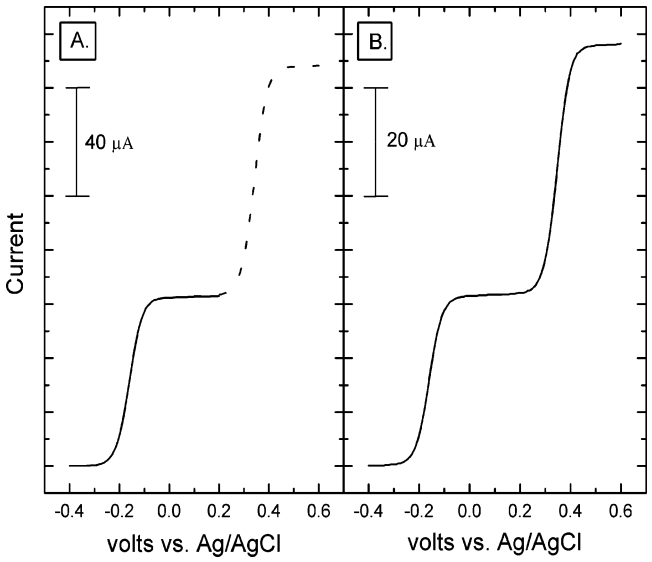

Figure 2. (A) NPV (using a Au disk electrode 0.0201 cm^2; pulse width, 50 ms; step time 1 s; potential increment 5 mV) of dMeFc (—, 3.10 mM) and Fc (- - -, 3.17 mM) in separate solutions of CH_3CN/0.1 M TBAP. The baseline of the Fc voltammogram has been offset from zero by an amount equal to the limiting current of dMeFc in order to simulate the expected voltammogram from the mixture of the two compounds. (B) Actual NPV after mixing equal volumes of the two solutions in (A).

dMeFc and another containing Fc in CH_3CN/0.1 M TBAP. The baseline of the Fc voltammogram (dashed line) has been offset from the zero-current baseline by an amount equal to the mass-transfer limited current of dMeFc. That operation furnishes an $i-E$ curve that shows the *expected* voltammogram of a mixture of dMeFc and Fc should eq 3 be obeyed.

Figure 2B shows the actual voltammogram of a mixture made of equal volumes of the two solutions of Figure 2A. Since the concentrations of both dMeFc and Fc have been halved, to keep the relative size of the voltammogram the same, the sensitivity of the current scale in Figure 2B has been doubled. By that operation, the relative size of the first wave (oxidation of dMeFc) remains the same.[15] Nevertheless, the second wave is larger than what is expected by simple superposition of the two currents, and therefore, eq 3 is not valid. From Figure 2A, it is calculated that the ratio $(i_{l,Fc}/i_{l,dMeFc})_{expected} = 1.34$ while from Figure 2B it is found that $(i_{l,Fc}/i_{l,dMeFc})_{mixture} = 1.47$. Based on the fact that the relative size of the first wave was not affected by the act of mixing, the current allocated for the oxidation of Fc appears ∼10% higher than expected from eq 3.

Although the phenomena of Figure 2 are reproducible, nevertheless, individual experiments cannot be compared directly, if for no other reason than just because the concentrations of Fc and dMeFc cannot be made exactly the same in all experiments. Therefore, to compare results from different experiments limiting-current data must be normalized. For this purpose, we use eq 6

$$\left(\frac{i_{l,R_2}}{i_{l,R_1}}\right)_N = \left(\frac{i_{l,R_2}}{i_{l,R_1}}\right)_{mixture} \left(\frac{D_{R_2}^{\beta} C_{R_2}^*}{D_{R_1}^{\beta} C_{R_1}^*}\right)^{-1} \qquad (6)$$

to define the normalized limiting-current ratio $(i_{l,R_2}/i_{l,R_1})_N$. Exponent β takes the value of $^1/_2$ for linear diffusion-controlled methods (SCV, NPV, CV, DPV) and $^2/_3$ in RDE voltammetry. The ratio $(i_{l,R_2}/i_{l,R_1})_{mixture}$ in eq 6 is equal to $(i_{2^{nd}plateau} - i_{l,R_1})/i_{l,R_1}$ and is calculated directly from the data of Figure 2B. Now, if eq 3 was valid $(i_{2^{nd}plateau} - i_{l,R_1})/i_{l,R_1} = (i_d - i_{l,R_1})/i_{l,R_1} = (i_{l,R_2}/i_{l,R_1})_{expected} = (D_{R_2}^{1/2} C_{R_2}^*/D_{R_1}^{1/2} C_{R1}^*)$, and clearly, the normalized ratio $(i_{l,R_2}/i_{l,R_1})_N$ would be equal to "1" for any combination of diffusion coefficients and concentrations. Conversely, the deviation of $(i_{l,R_2}/i_{l,R_1})_N$ from unity should quantify the effect of eq 4 with no reference to the particular experiment. Now, since $(D_{R_2}^{1/2} C_{R_2}^*/D_{R1}^{1/2} C_{R1}^*) = (i_{l,R_2}/i_{l,R_1})_{expected}$, which is determined experimentally from the data of Figure 2A, eq 6 is modified into eq 7, where both right-hand side

$$\left(\frac{i_{l,R_2}}{i_{l,R_1}}\right)_N = \left(\frac{i_{l,R_2}}{i_{l,R_1}}\right)_{mixture} \left(\frac{i_{l,R_2}}{i_{l,R_1}}\right)_{expected}^{-1} \qquad (7)$$

quantities are taken directly from Figure 2. Note also that, for RDE voltammetry, where $\beta = ^2/_3$, the corresponding quantity $D_{R_2}^{2/3} C_{R_2}^*/D_{R_1}^{2/3} C_{R_1}^*$ is again equal to $(i_{l,R_2}/i_{l,R_1})_{expected}$, and therefore, eq 7 is valid for any voltammetric method.[16]

At this point, it should be noted that, by definition, the $(i_{l,R_2}/i_{l,R_1})_N$ ratio reflects the electroanalytical use of voltammetry: i_{l,R_1} may represent the limiting current from an analyte and i_{l,R_2} the limiting current from an internal standard, or vice versa. The ratio $\rho = i_{d,experimental}/i_{d,theoretical}$, used by Andrieux et al.,[11] that is the ratio of the experimental second current plateau over the second

(15) The current allocated to the oxidation of dMeFc in the mixture is within 1.6% of half the current produced by the oxidation of dMeFc by itself before mixing.

(16) We thank the reviewer who suggested the generalization of eqs 6 and 7 in terms of exponent β.

Table 2. Normalized Mass-Transfer Limited Current Ratios $(i_{l,R_2}/i_{l,R_1})_N$ for the dMeFc/Fc System (R_1 = dMeFc, R_2 = Fc)

	By NPV/SCV[a] τ				
	50 ms	100 ms	1 s	2 s	3 s
NPV	1.10 ± 0.01 (4)	1.09 ± 0.00 (4)			
SCV	1.11 ± 0.01 (3)	1.08 ± 0.01 (3)	1.08 ± 0.02 (3)	1.08 ± 0.00 (3)	1.08 ± 0.01 (3)

By RDE Voltammetry[b] ω					
50 rpm	100 rpm	200 rpm	600 rpm	1000 rpm	1400 rpm
$1.08_5 \pm 0.00_5$	$1.07_5 \pm 0.00_5$	1.09 ± 0.00	1.09 ± 0.01	$1.08_5 \pm 0.00_5$	$1.09_5 \pm 0.00_5$

[a] In parentheses are the number of independent experiments used for averaging. The error is the spread between the high and the low values. [b] Average values from two experiments. Again, the error is the spread between the high and the low values.

current plateau if the reaction of eq 4 was not present, does not contain any information about the relative limiting currents from the analyte and the internal standard. In fact, the two ratios, $(i_{l,R_2}/i_{l,R_1})_N$ and ρ, are not mathematically equivalent (i.e., $(i_{l,R_2}/i_{l,R_1})_N$ cannot be derived from ρ), and as discussed below in the section entitled Role of the Rate Constant k_f and the Bulk Concentration Ratio $C_{R_1}^*/C_{R_2}^*$ on $(i_{l,R_2}/i_{l,R_1})_N$ (see also ref 26), the latter has some other theoretical limitations too.

Table 2 presents the values of the experimentally determined $(i_{l,R_2}/i_{l,R_1})_N$ ratio for the dMeFc/Fc system at 0.05 and 0.1 s by NPV and at 0.05, 0.1, 1, 2, and 3 s by SCV. (Although NPV and SCV are conceptually identical methods, for practical reasons, sampling times in the range of 1−3 s were employed only with SCV.) At the two common sampling times (50 and 100 ms), the $(i_{l,R_2}/i_{l,R_1})_N$ ratio is within error equal by the two methods, and there is no statistically significant variation in the value of that ratio for $\tau \geq 100$ ms.

The phenomena of Figure 2 are quite general. Figure 3B, for example, shows that the second wave in the cyclic voltammogram of a dMeFc/Fc mixture is larger than what is expected by simple superposition of the cyclic voltammograms of the two components (Figure 3A). Similarly, Figure 4B shows that the peak current of Fc in the differential pulse voltammogram of the mixture is higher than the peak current expected by simple superposition of the individual DPVs (Figure 4A). The error in the second peak height in the mixture is ∼13%.

The phenomena demonstrated up to this point are not limited to diffusion-controlled methods. Figure 5 shows analogous results obtained with a rotating electrode. Using the relative size of the first wave as reference, the second wave appears ∼10% higher in the mixture than what is expected by simple superposition. The values of the $(i_{l,Fc}/i_{l,dMeFc})_N$ ratio (eq 7) for the system of Figure 5 have been also tabulated in Table 2 for different rotation rates ranging from 50 to 1400 rpm. The values of the $(i_{l,Fc}/i_{l,dMeFc})_N$ ratio are within error equal to the values of the same ratio determined by NPV/SCV and remain constant over the range of the electrode rotation rates, ω, considered.

$[Co(bipy)_3]^{2+}$/*N*-Methylphenothiazine System. Qualitatively, identical observations made with the dMeFc/Fc pair are also prevalent here. Data for different sampling times and rotation rates are summarized in Table 3. The behavior of the $[Co(bipy)_3]^{2+}$/MePTZ pair under diffusion control is shown in Figure 6 using SCV. By both SCV/NPV and RDE voltammetry, the second wave in the mixture (corresponding to the oxidation of MePTZ) is higher (by ∼20%) than expected from eq 3. It is noted further that the values of the $(i_{l,MePTZ}/i_{l,Co(II)})_N$ ratio are higher at shorter sampling times and faster rotation rates, decreasing at longer sampling times and slower rotation rates toward a common limiting value. This observation is counterintuitive, because one would have expected that as $(i_{l,MePTZ}/i_{l,Co(II)})_N$ deviates from unity, its limiting value should have been reached from lower values, not higher.

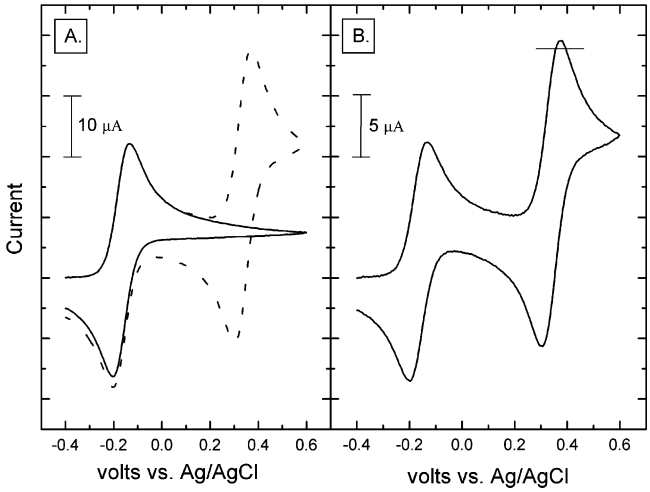

Figure 3. (A) CV (at 0.1 V s^{-1}, with a Au disk electrode 0.0201 cm^2) of dMeFc (—, 3.03 mM) and Fc (3.12 mM) in separate solutions of CH_3CN/0.1 M TBAP. The dashed line (- - -) is the sum of the two voltammograms and simulates the expected voltammogram of the mixture. (B) Actual CV after mixing equal volumes of the two solutions in (A). The horizontal line near the second peak shows the expected current in the absence of eq 4.

In summary, by using two randomly selected pairs of redox-active substances, we have shown that voltammetric currents are not additive. Therefore, we conclude that the same statement is expected to hold true for any other mixture of redox-active substances. In the ensuing discussion we seek to identify the conditions under which currents *are* additive and, in the general case that they are not, to study the role of the controlling parameters and to propose methodology for correcting electroanalytical data.

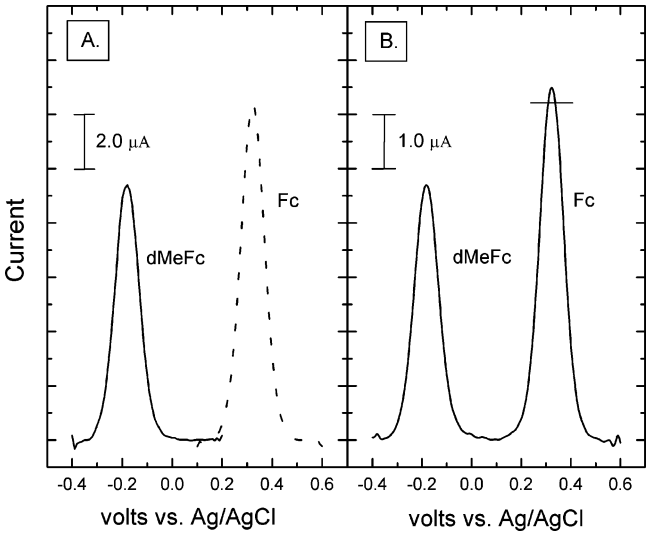

Figure 4. DPV (pulse width 100 ms; step time 2 s; pulse height 25 mV; potential increment 10 mV) of the same solutions and the same experimental sequence used in Figure 3.

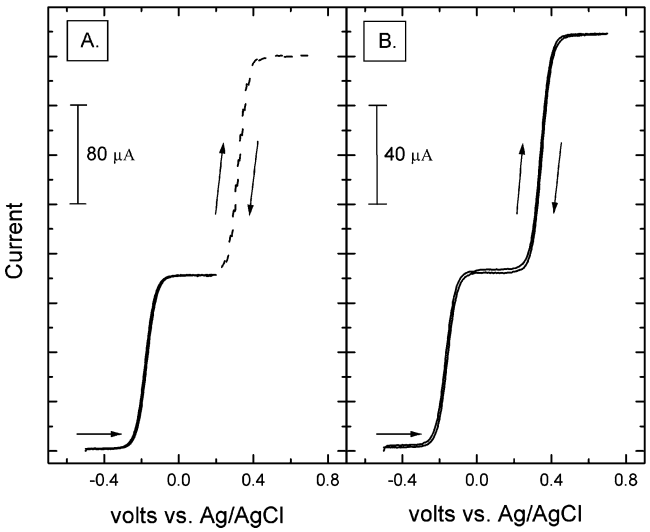

Figure 5. (A) RDE voltammetry (100 rpm, 0.01 V s^{-1}, with a Au disk electrode 0.0412 cm^2) of dMeFc (—, 3.02 mM) and Fc (- - -, 3.05 mM) in separate solutions of CH_3CN/0.1 M TBAP. The baseline of the Fc voltammogram has been offset from zero as described in the legend of Figure 2. (B) Actual RDE voltammogram after mixing equal volumes of the two solutions in (A).

DISCUSSION

The purpose of this section is to describe quantitatively the chemical system defined by eqs 1, 2, and 4, confirm the experimental results from a theoretical standpoint, and use the conclusion for making specific suggestions for experimental design and data analysis. To avoid unnecessary confusion due to the experimental method the chemical system is probed with, we will concentrate on millielectrode-based SCV, a method where mass transfer is controlled by linear diffusion. For convective-diffusion-controlled methods like RDE voltammetry, we have shown recently that (a) convection compresses diffusion-like concentration profiles close to the electrode, leaving *relative* fluxes—and faradaic currents—unaffected, and (b) in the presence of comproportionation (eq 5), faster rotation rates of the RDE correspond to shorter sampling times in SCV as in both cases the diffusion layer is thinner and thus the time allowed for eq 4 becomes shorter.[5] Therefore, at first approximation, conclusions drawn from a discussion centered on SCV can be extrapolated into RDE voltammetry readily.

Our first objective is to identify the conditions that validate eq 3. At the potential range where both reactions 1 and 2 take place simultaneously, the faradaic current i is given by eq 8 in terms of

$$i = FAD_{R_1}(\partial C_{R_1}/\partial x)_{x=0} + FAD_{R_2}(\partial C_{R_2}/\partial x)_{x=0} \qquad (8)$$

the sum of the fluxes of R_1 and R_2 at the electrode (x is the distance from the electrode).[1] Therefore, to discuss the effect of eq 4 on i, we must investigate its effect on the concentration profiles, C_{R_1} and C_{R_2}. Under linear diffusion, the space−time evolution of C_{R_1} and C_{R_2} is described by eqs 9 and 10, where t is the time and k_f

$$\frac{\partial C_{R_1}}{\partial t} = D_{R_1}\frac{\partial^2 C_{R_1}}{\partial x^2} - k_f C_{R_1} C_{O_2} + k_b C_{R_2} C_{O_1} \qquad (9)$$

$$\frac{\partial C_{R_2}}{\partial t} = D_{R_2}\frac{\partial^2 C_{R_2}}{\partial x^2} + k_f C_{R_1} C_{O_2} - k_b C_{R_2} C_{O_1} \qquad (10)$$

and k_b are the rate constants of the forward and backward reactions in eq 4.

In close analogy to Evans' analysis of the voltammetric effects of eq 5,[3] it is noted that if eqs 9 and 10 are added, the kinetic terms are removed (eq 11), and if $D_{R_1} = D_{R_2}$, eq 11 can be recast

$$\frac{\partial C_{R_1}}{\partial t} + \frac{\partial C_{R_2}}{\partial t} = D_{R_1}\frac{\partial^2 C_{R_1}}{\partial x^2} + D_{R_2}\frac{\partial^2 C_{R_2}}{\partial x^2} \qquad (11)$$

$$\frac{\partial C_R}{\partial t} = D_R\frac{\partial^2 C_R}{\partial x^2} \qquad (12)$$

into eq 12, where $C_R = C_{R_1} + C_{R_2}$ and D_R is the common value of D_{R_1} and D_{R_2}.

The initial ($t = 0$) condition for eq 12 applies at all x ($\forall x$) and is given by

$$C_R|_{t=0,\forall x} = C^*_{R_1} + C^*_{R_2} \qquad (13)$$

The boundary conditions of eq 12 at the mass-transfer limited second current plateau are

$$\text{at the electrode } (x{=}0): \quad C_R|_{\forall t, x=0} = 0 \qquad (14)$$

$$\text{in the bulk } (x\rightarrow\infty): \quad C_R|_{\forall t, x\rightarrow\infty} = C^*_{R_1} + C^*_{R_2} \qquad (15)$$

The system of eqs 12−15 comprise a diffusion problem, uncomplicated by kinetics, where the chronoamperometric current at a certain sampling time τ is given by eq 16, which is identical

$$i = \frac{FAD_R^{1/2}(C^*_{R_1} + C^*_{R_2})}{\pi^{1/2}\tau^{1/2}} \qquad (16)$$

Table 3. Normalized Mass-Transfer Limited Current Ratios $(i_{l,R_2}/i_{l,R_1})_N$ for the $[Co(bipy)_3]^{2+}$/MePTZ System (R_1 = $[Co(bipy)_3]^{2+}$, R_2 = MePTZ)[a]

	by NPV/SCV τ					
	25 ms	50 ms	100 ms	1 s	2 s	3 s
NPV	$1.21_5 \pm 0.00_5$ (2)	$1.19_0 \pm 0.00_7$ (4)	$1.18_5 \pm 0.01_5$ (4)			
SCV	1.22 ± 0.02 (2)	$1.21_3 \pm 0.00_4$ (4)	$1.17_8 \pm 0.01_1$(4)	$1.17_5 \pm 0.00_5$ (2)	1.18 ± 0.00 (2)	1.18 ± 0.01 (2)

	By RDE voltammetry[a] ω						
50 rpm	100 rpm	200 rpm	600 rpm	1000 rpm	1400 rpm	1800 rpm	2000 rpm
$1.18_5 \pm 0.00_5$ (2)	$1.17_5 \pm 0.00_5$ (2)	1.18 ± 0.01 (2)	$1.19_5 \pm 0.00_5$ (2)	1.21 ± 0.01 (2)	1.22 ± 0.01 (2)	1.22 ± 0.01 (2)	1.24 ± 0.00 (2)

[a] In parentheses is the number of independent experiments used for averaging. When that number is 2, the error is the spread between the high and the low values; when it is 4 the error is the standard deviation.

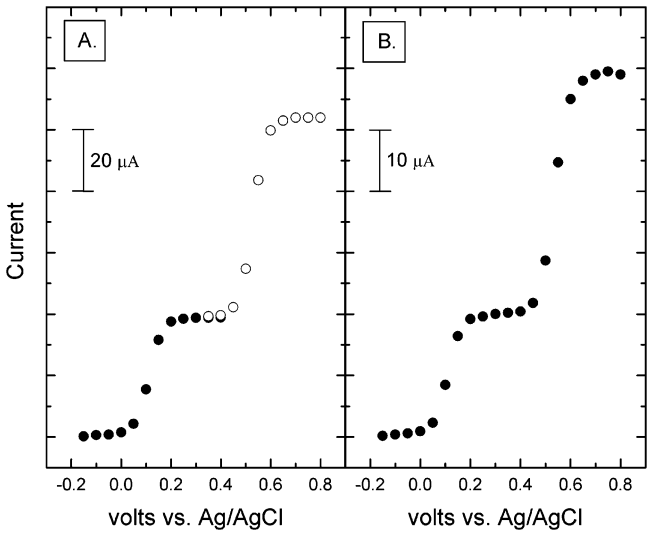

Figure 6. (A) SCV (τ = 50 ms, with a Au disk electrode 0.0201 cm^2) of $[Co(bipy)_3]^{2+}$ (solid circles, 2.99 mM) and of MePTZ (open circles, 3.18 mM) in separate solutions of CH_3CN/1.0 M $LiClO_4$. The baseline of the MePTZ voltammogram has been offset from zero in order to simulate the voltammogram of the mixture. Actual SCV after mixing equal volumes of the two solutions in (A). (In all SCV experiments, initial conditions between each potential step were reestablished by stirring the solution.)

to eq 3 for $D_{R_1} = D_{R_2}$. If the latter condition is not fulfilled, eqs 9 and 10 cannot be combined. In that case, the current expected from a mixture of R_1 and R_2 must be calculated via eqs 9 and 10, which are solved together with eqs 17 and 18 that describe the

$$\frac{\partial C_{O_1}}{\partial t} = D_{O_1}\frac{\partial^2 C_{O_1}}{\partial x^2} + k_f C_{R_1} C_{O_2} - k_b C_{R_2} C_{O_1} \qquad (17)$$

$$\frac{\partial C_{O_2}}{\partial t} = D_{O_2}\frac{\partial^2 C_{O_2}}{\partial x^2} - k_f C_{R_1} C_{O_2} + k_b C_{R_2} C_{O_1} \qquad (18)$$

evolution of C_{O_1} and C_{O_2}, as well as the appropriate initial conditions (eq 19) and boundary conditions (eqs 20−22).

$$C_{R_1}|_{t=0,\forall x} = C^*_{R_1}, \quad C_{R_2}|_{t=0,\forall x} = C^*_{R_2}, \quad C_{O_1}|_{t=0,\forall x} = C_{O_2}|_{t=0,\forall x} = 0 \qquad (19)$$

At the electrode ($\forall t$, x=0), assuming that both redox reactions are Nernstian[17]

$$E = E^{\circ\prime}_{O_1/R_1} + \frac{RT}{F}\ln\frac{C_{O_1}|_{\forall t,x=0}}{C_{R1}|_{\forall t,x=0}} \quad \text{and}$$

$$D_{R_1}\left(\frac{\partial C_{R_1}}{\partial x}\right)_{\forall t,x=0} + D_{O_1}\left(\frac{\partial C_{O_1}}{\partial x}\right)_{\forall t,x=0} = 0 \qquad (20)$$

$$E = E^{\circ\prime}_{O_2/R_2} + \frac{RT}{F}\ln\frac{C_{O_2}|_{\forall t,x=0}}{C_{R_2}|_{\forall t,x=0}} \quad \text{and}$$

$$D_{R_2}\left(\frac{\partial C_{R_2}}{\partial x}\right)_{\forall t,x=0} + D_{O_2}\left(\frac{\partial C_{O_2}}{\partial x}\right)_{\forall t,x=0} = 0 \qquad (21)$$

In the bulk ($\forall t$, $x \to \infty$)

$$C_{R_1}|_{\forall t,x\to\infty} = C^*_{R_1}, \quad C_{R_2}|_{\forall t,x\to\infty} = C^*_{R_2}, \quad C_{O_1}|_{\forall t,x\to\infty} = C_{O_2}|_{\forall t,x\to\infty} = 0 \qquad (22)$$

In its most general form, the nonlinear system of eqs 9, 10, and 17−22 cannot be solved analytically. Instead, it was solved numerically following an explicit finite difference integration method.[5,19] The only simplification made was to omit the terms containing k_b. This is justified by the fact that $K = k_f/k_b$, and since internal standards are chosen so that their waves are well-separated from the waves of the analytes, the equilibrium constant K is large, and therefore, $k_f \gg k_b$.

Figure 7 shows simulated sampled current voltammograms for the $[Co(bipy)_3]^{2+}$/MePTZ system in the same format as the experimental data of Figure 6. The concentrations of the two components were set equal to one another (at 1 mM), and the diffusion coefficients of all species involved were taken from Table 1. The rate constant k_f was set equal either to 0 or to 10^7 M^{-1} s^{-1}, and sampling of the Cottrell current was set at 50 ms after

(17) For instance, the $[Co(bipy)_3]^{3+/2+}$ redox couple is quasi-reversible,[18] but this fact is inconsequential from the viewpoint of this discussion that concerns only mass-transfer limited currents.

(18) Williams, M. E.; Crooker, J. C.; Pyati, R.; Lyons, L. J.; Murray, R. W. *J. Am. Chem. Soc.* **1997**, *119*, 10249.

(19) Feldberg, S. W. In *Electroanalytical Chemistry. A Series of Advances*; Bard, A. J., Ed.; Marcel Dekker: New York, 1969; Vol. 3, p 199.

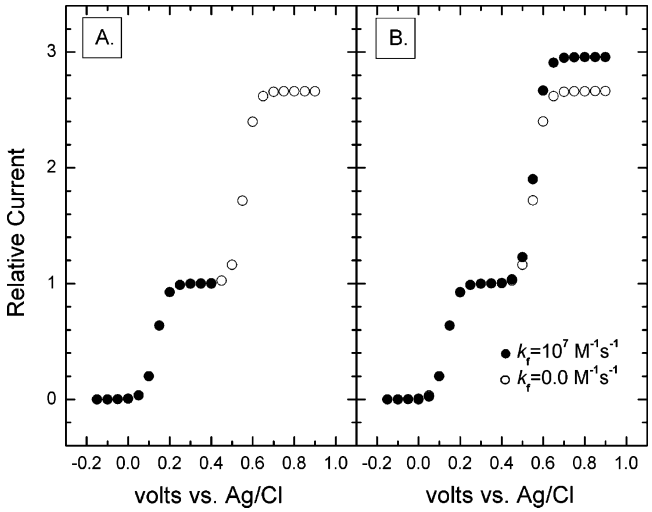

Figure 7. (A) Simulated SCV (τ = 50 ms) of $[Co(bipy)_3]^{2+}$ (solid circles) and MePTZ (open circles) both at 1 mM in separate solutions. The baseline of the MePTZ voltammogram has been offset as described in the legend of Figure 6. ($E^{\circ\prime}_{Co^{III/II}}$ = 0.136 V vs Ag/AgCl; $E^{\circ\prime}_{MePTZ^{\bullet+/0}}$ = 0.555 V vs Ag/AgCl.) (B) Simulated SCV (τ = 50 ms) of a mixture containing equal concentrations (1 mM) of $[Co(bipy)_3]^{2+}$ and MePTZ at two different reaction rates.

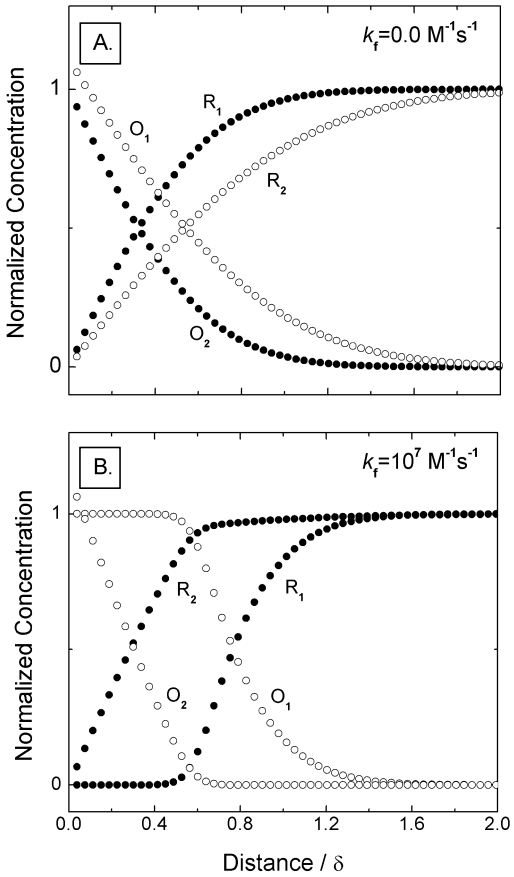

Figure 8. Concentration profiles at the second current plateau of the simulated voltammograms of Figure 7B. $R_1 = [Co(bipy)_3]^{2+}$, R_2 = MePTZ, $O_1 = [Co(bipy)_3]^{3+}$, and O_2 = MePTZ$^{\bullet+}$. $C^*_{R_1} = C^*_{R_2}$ (1.0 mM). Concentrations have been normalized to the common bulk concentration of R_1 and R_2. The profiles are also invariant of time, as the distance from the electrode is given in multiples of the diffusion layer thickness, δ ($= \pi^{1/2}\tau^{1/2}D^{1/2}_{MePTZ}$).[1] Here, δ = 16.1 μm.

every potential step. By comparing parts A and B of Figure 7, it is noted that if k_f were equal to zero (i.e., in the absence of eq 4) the voltammogram of the mixture would be predictable by simple superposition of the voltammograms of each component, and $(i_{l,MePTZ}/i_{l,Co(II)})_N = 1$. If $k_f = 10^7$ M^{-1} s^{-1}, the computed voltammogram resembles the experimental one (compare Figures 6B and 7B), and within the uncertainty in the diffusion coefficients (Table 1), the computed value of the $(i_{l,MePTZ}/i_{l,Co(II)})_N$ ratio (1.177) is also equal to the limiting value of that ratio at long sampling times ($\tau \geq$ 100 ms—see Table 3).

Computed concentration profiles of all four species R_1, R_2, O_1, and O_2 at the second current plateau are shown in Figure 8 for k_f = 0.0 M^{-1} s^{-1} and for $k_f = 10^7$ M^{-1} s^{-1}. Those profiles conform with concentration profiles traced recently by Amatore et al. using a UME probe in the vicinity of an electrode where fluorenone and L-cyanonaphthalene undergo simultaneously one-electron reductions.[20] As expected, in the presence of eq 4 (Figure 8B), R_1 is replaced by R_2 and does not reach the electrode. Since the diffusion coefficient of R_2 (i.e., of MePTZ in this particular case) is ~2.8 times higher than the diffusion coefficient of the Co(II) complex (R_1), the resulting flux of oxidizable equivalents to the electrode is higher than what it would have been in the absence of eq 4. Hence the mass-transfer limited current is increased. These results mandate a more systematic study of the influence of the diffusion coefficients on the $(i_{l,MePTZ}/i_{l,Co(II)})_N$ ratio. That task, however, should be part of a more general analysis of the system of eqs 9, 10, and 17−22 as a function of the controlling parameters that include not only the diffusion coefficients but also the rate constant, k_f and the initial (bulk) concentrations of R_1 and R_2. For reasons that will become apparent shortly, that analysis starts from k_f.

(1) Role of the Rate Constant k_f and the Bulk Concentration Ratio $C_{R_1}^*/C_{R_2}^*$ on $(i_{l,R_2}/i_{l,R_1})_N$. In this section, we investigate the variation of the computed value of the $(i_{l,R_2}/i_{l,R_1})_N$ ratio as k_f varies from zero to 10^7 M^{-1} s^{-1}. (Again, as our model we will use the $[Co(bipy)_3]^{2+}$/MePTZ system.) This investigation is important for two reasons: (a) We have been intrigued by the fact that at earlier sampling times (e.g., at τ = 50 ms) and at faster rotation rates (e.g., at ω = 2000 rpm) the experimentally obtained $(i_{l,MePTZ}/i_{l,Co(II)})_N$ ratio is *higher* than its value at longer τ's and slower ω's (see Table 3). Therefore, we are forced to conclude that the $(i_{l,MePTZ}/i_{l,Co(II)})_N$ ratio does *not* vary monotonically from unity (i.e., its value for k_f = 0) to its limiting value at large k_f's. This deduction is counterintuitive, and since our system is intractable analytically it must be confirmed computationally. (b) We reasoned, in analogy to our previous studies of comproportionation reactions,[5] that by sampling the current at earlier times after each potential step eq 4 would be allowed to proceed for a shorter period of time before the system is questioned; thereby a relatively low value of k_f could lead to an incomplete reaction and the $(i_{l,R_2}/i_{l,R_1})_N$ ratio would be closer to unity. In turn, that would allow for a kinetic evaluation of eq 4.

Figure 9 shows the value of the calculated $(i_{l,R_2}/i_{l,R_1})_N$ ratio as k_f is varied from zero to 10^7 M^{-1} s^{-1}. Calculations have been performed for equal concentrations (1 mM) of the Co(II) complex and MePTZ, and the different curves correspond to different sampling times. In agreement with the conceptual association of

(20) Amatore, C.; Szunerits, S.; Thouin, L.; Warkocz, J.-S. *Electroanalysis* **2001**, *13*, 646.

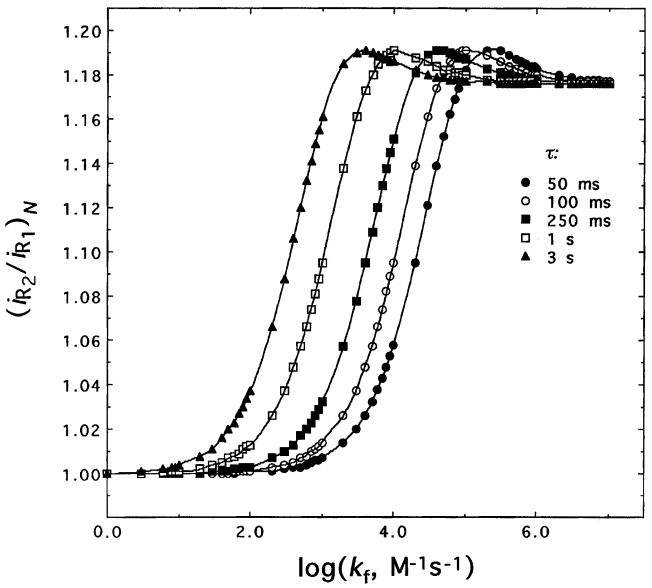

Figure 9. Dependence of the $(i_{l,R_2}/i_{l,R_1})_N$ ratio on the forward rate constant of eq 4 (k_f) at different sampling times, τ. (The diffusion coefficients used for these simulations are those for the $[Co(bipy)_3]^{2+}$/MePTZ system. $C^*_{R_1}/C^*_{R_2} = 1$. Note also that if $(i_{l,R_2}/i_{l,R_1})_N$ is plotted vs $\log(k_f\tau)$, all five curves will coalesce.)

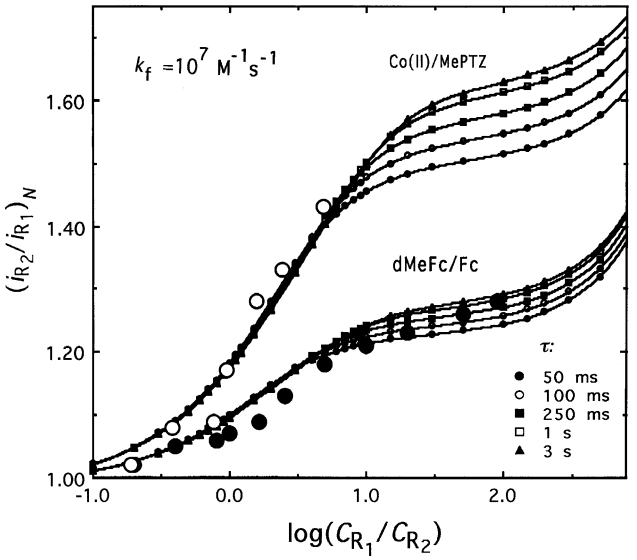

Figure 10. Simulated variation of the $(i_{l,R_2}/i_{l,R_1})_N$ ratio as a function of the relative bulk concentrations of R_1 and R_2. (Upper cluster curves: $R_1 = [Co(bipy)_3]^{2+}$, R_2 = MePTZ. Lower cluster curves: R_1 = dMeFc, R_2 = Fc. Note also that if the $(i_{l,R_2}/i_{l,R_1})_N$ ratio were calculated at constant $k_f\tau$ values, rather than constant k_f's, each cluster of curves would coalesce into a single line.) Large solid circles: experimental data with the dMeFc/Fc system. Large open circles: experimental data with the $[Co(bipy)_3]^{2+}$/MePTZ system. (The radii of the circles extend one standard deviation from the average values.)

reaction completion and sampling time, for longer sampling times, the $(i_{l,R_2}/i_{l,R_1})_N$ ratio departs from unity quickly and reaches its long-τ limiting value (1.176) at lower values of k_f. Furthermore, it is also noted that the $(i_{l,R_2}/i_{l,R_1})_N$ ratio does not reach its high k_f limit monotonically: As k_f increases, $(i_{l,R_2}/i_{l,R_1})_N$ goes through a maximum and then decreases again, approaching its high-k_f limit from above. This confirms the experimental observations of Table 3, and from this viewpoint, the rate constant k_f for the reaction of $MePTZ^{\bullet+}$ with $[Co(bipy)_3]^{2+}$ should be in the range of 10^6-10^7 M^{-1} s^{-1}. The value calculated via the Marcus expression $k_f \simeq (k_{11}k_{22}K)^{1/2}$ is 1.1×10^7 M^{-1} s^{-1}.[21,22]

Now, the nonmonotonic variation of the $(i_{l,R_2}/i_{l,R_1})_N$ ratio with k_f is difficult to reconcile. We attribute it to the nonlinearity of the system of eqs 9, 10, and 17−22, and in that context, it is noted that due to the semi-infinite boundary conditions (eq 22) that system of equations never reaches a steady state. But if it could reach a steady state (i.e., if $\partial C_i/\partial t = 0$, $\forall i$), then that system of equations would fulfill the necessary condition for chaotic dynamics.[24] Under those circumstances, the concentration profiles could depend strongly on the initial conditions. That line of reasoning prompted us to look into the effect of the relative bulk concentrations of R_1 and R_2 on the value of $(i_{l,R_2}/i_{l,R_1})_N$. Indeed, Figure 10 shows that the limiting value of the $(i_{l,R_2}/i_{l,R_1})_N$ ratio at high k_f's does vary as a function of the relative bulk concentrations of R_1 and R_2 $(C^*_{R_1}/C^*_{R_2})$.[26] The computed results of Figure 10 were confirmed experimentally in the concentration range $0.1 \le C^*_{R_1}/C^*_{R_2} \le 100$, and the data are also included in that figure. Those results signify that the calibration factor of an oxidizable (reducible) single-component system with an oxidizable (reducible) internal standard is not constant, and therefore, calibration curves over extended concentration ranges are expected to be nonlinear. (Of course, calibration of a multiple-component system is completely futile due to all conceivable combinations of eq 4.)

(2) Role of the Diffusion Coefficients on $(i_{l,R_2}/i_{l,R_1})_N$. We have worked with equal concentrations of R_1 and R_2 at the high-k_f limit (10^7 M^{-1} s^{-1}) where the $(i_{l,R_2}/i_{l,R_1})_N$ ratio reaches a limiting value for all sampling times used both experimentally and computationally. Figure 11 shows how that ratio varies as a function of D_{R_1}/D_{R_2} and D_{R_2}/D_{O_2}. (The computer-generated data used for Figure 11 are given in Supporting Information as Appendix S.I) Since R_1 is replaced by R_2 (Figure 8), it is not surprising that the value of the $(i_{l,R_2}/i_{l,R_1})_N$ ratio is most sensitive to the D_{R_1}/D_{R_2} ratio (Figure 11). Meanwhile, the flux of R_2 is coupled (via eq 21) to the flux of O_2, which in turn depends on

(21) Marcus, R. A.; Sutin, N. *Biochim. Biophys. Acta* **1985**, *811*, 265−322.

(22) k_{11} is the self-exchange rate constant of the $[Co(bipy)_3]^{3+} + [Co(bipy)_3]^{2+}$ system (18 M^{-1} s^{-1}),[21] k_{22} is the same constant of the $MePTZ^{\bullet+}$ + MePTZ system, (~5×10^5 M^{-1} s^{-1}, measured in films),[23] and K is the equilibrium constant of eq 4 (1.3×10^7).

(23) Morishiwa, Y.; Akihara, I.; Lim, H. S.; Nozakura, S. *Macromolecules* **1987**, *20*, 978.

(24) A set of at least three differential equations nonlinearly coupled.τ

(25) τ.Baker, G. L.; Gollub, J. P. *Chaotic Dynamics An Introduction*; Cambridge University Press: New York, 1990, Chapter 1.

(26) Importantly, the ρ $(= i_{d,experimental}/i_{d,theoretical})$ ratio used in ref 11 to describe effects from eq 4-type reactions varies also with the concentration ratio $C^*_{R_1}/C^*_{R_2}$ and yields a bell-shaped curve, whose high- and low-end limits are both equal to unity (i.e., at both ends, lim $\rho = 1$), irrespective of eq 4. Indeed, again let i_{l,R_1} be the limiting current from the first wave, which is always unaffected by eq 4; let i^{exp}_{l,R_2} be the actual experimental current of the second wave; and, let i^{hyp}_{l,R_2} be the hypothetical current of the second wave if eq 4 were not present. Then, by definition $\rho = (i_{l,R_1} + i^{exp}_{l,R_2})/(i_{l,R_1} + i^{hyp}_{l,R_2})$, and for $C^*_{R_2} \to 0$, both $i^{exp}_{l,R_2} \to 0$ and $i^{hyp}_{l,R_2} \to 0$ and therefore $\rho \to 1$. Likewise, for $C^*_{R_1} \to 0$, $i_{l,R_1} \to 0$, and necessarily $i^{exp}_{l,R_2} = i^{hyp}_{l,R_2}$, so again $\rho \to 1$. Clearly, the independence of ρ on eq 4 at high and low $C^*_{R_1}/C^*_{R_2}$ ratios gives the incorrect impression that the effects of eq 4 are not present. On the other hand, it is not obvious to us at all how the $i^{exp}_{l,R_2}/i^{hyp}_{l,R_2}$ ratio (which is equal to the $(i_{l,R_2}/i_{l,R_1})_N$ ratio that has been used throughout this study) varies as a function of the $C^*_{R_1}/C^*_{R_2}$ ratio. The only way we could elucidate that dependence was through digital simulations, and the results were confirmed experimentally (see Figure 10).

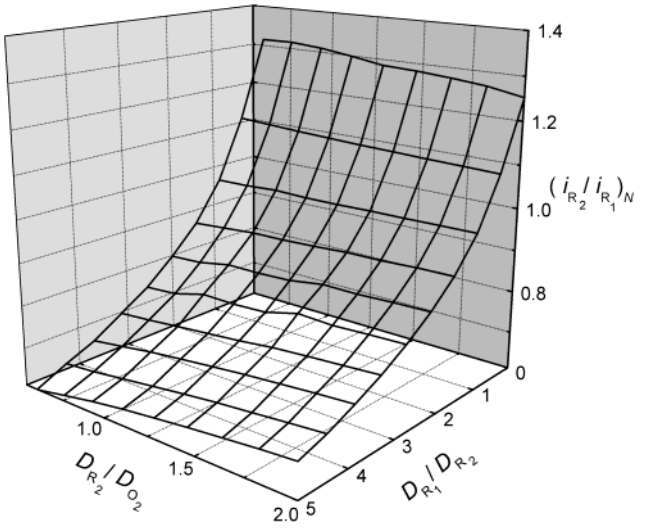

Figure 11. Variation of the $(i_{l,R_2}/i_{l,R_1})_N$ ratio by simulated SCV (τ = 50 ms) as a function of the diffusion coefficient ratios D_{R_1}/D_{R_2}, D_{R_2}/D_{O_2}. $k_f = 10^7$ M^{-1} s^{-1}. $(C^*_{R_1}/C^*_{R_2}) = 1$.

D_{O_2}. Therefore, a weaker sensitivity of $(i_{l,R_2}/i_{l,R_1})_N$ on the D_{R_2}/D_{O_2} ratio is not difficult to reconcile either. Along the same line of reasoning, $(i_{l,R_2}/i_{l,R_1})_N$ is insensitive within the accuracy of the data of Appendix S.1 to the D_{R_1}/D_{O_1}ratio, and the data are not shown.

Appendix S.I can be used in lieu of simulations in order to find the value of the $(i_{l,R_2}/i_{l,R_1})_N$ ratio. In turn, that ratio can be used as a calibration factor with the understanding that the value of the $C^*_{R_1}/C^*_{R_2}$ ratio must be close to unity. Indeed, for the dMeFc/Fc system for instance, $D_{dMeFc}/D_{Fc} = 0.60$ and $D_{Fc}/D_{Fc^{\bullet+}} = 1.05$ (Table 1). Then from Appendix S.I we find that, for this combination of diffusion coefficients, the value of $(i_{l,R_2}/i_{l,R_1})_N$ is ~1.098, which is also equal to the experimentally determined ratio (refer to Table 2). Similarly, for the $[Co(bipy)_3]^{2+}$/MePTZ system, using data from Table 1 and Appendix S.I it is estimated that at the long-τ limit $(i_{l,R_2}/i_{l,R_1})_N \sim 1.179$. This value is again equal to the experimental (Table 3) and the computed (Figure 7) ratio.

(3) Role of Eq 4 on the Half-Wave Potentials, $E_{1/2}$. A curious observation came up during analysis of simulated voltammograms such as those in Figure 7B: It was noted that during resizing of the second wave, its midpoint potential (i.e., its $E_{1/2}$) is shifted slightly in the negative direction; that is, the two waves come somewhat closer to one another. For the sake of clarity, Appendixes S.II and S.III in Supporting Information present overlapping simulated voltammograms for $k_f = 10^7$ M^{-1} s^{-1} and $k_f = 0.0$ M^{-1} s^{-1}, namely, in the presence and absence of the reaction of eq 4, and emphasize the $E_{1/2}$ region of the second wave for both systems considered in this study (dMeFc/Fc and $[Co(bipy)_3]^{2+}$/MePTZ).

Semiquantitatively, considering that eq 4 replaces O_2 and R_1 with R_2 and O_1, and that $E_{1/2}(2) = E^{o\prime}(2) - (RT/nF)\ln[(D_{O_2})^{1/2}/(D_{R_2})^{1/2}]$, the correction in the $E_{1/2}$ is expected to be in the order of magnitude of the $(RT/nF)\ln[(D_{O_2})^{1/2}/(D_{R_2})^{1/2}]$ term, namely, in the vicinity of 1 mV in the case of the dMeFc/Fc system and ~3 mV in the case of the $[Co(bipy)_3]^{2+}$/MePTZ system. The digital simulations of Appendixes S.II and S.III yield a negative shift of 1.88 mV for the $E_{1/2}$ of Fc in the dMeFc/Fc system and a negative shift of 2.94 mV for the $E_{1/2}$ of MePTZ in the $[Co(bipy)_3]^{2+}$/MePTZ system.

Because of the wide use of ferrocene as an internal electrochemical potential reference, those results were tested experimentally as follows: using dimethyl viologen (*N*,*N*′-dimethyl-4,4′-bipyridinium perchlorate), i.e., a reducible redox-active substance, as internal standard and NPV (at τ = 100 ms) as the electrochemical technique, it was found that the $\Delta E_{1/2}$ value between dMeFc and Fc was 507 mV before mixing and 504 mV after mixing the dMeFc and the Fc solutions together. (The $E_{1/2}$ value of dMeFc vs dimethyl viologen was +0.323 mV before mixing and +0.322 mV after mixing.) Using nitrobenzene as the reducible internal standard and CV (at 0.1 V s^{-1}) as the electrochemical method, it was found that the $\Delta E_{1/2}$ value between dMeFc and Fc was 506.5 mV before mixing and 501 mV after mixing the dMeFc and the Fc solutions together. (The $E_{1/2}$ value of dMeFc vs nitrobenzene was the same before and after mixing, at +1039 mV.)

CONCLUSIONS

Our results suggest that the accuracy of voltammetric methods of analysis may be compromised seriously by the homogeneous reaction of eq 4. Use of internal standards may complicate the situation even further by introducing new reactions of the same type. From that perspective, the ideal internal standard for oxidizable analytes should be a reducible redox-active compound. In other words, none of the compounds considered in this study could comprise a satisfactory internal standard for any of the others. Instead, an acceptable internal standard for any one of those compounds could be a well-characterized reducible species such as *N*,*N*′-dimethyl viologen, or nitrobenzene.

If one has to choose an oxidizable internal standard for an oxidizable analyte, the primary concern should be to match closely diffusion coefficients and concentrations of the two species. If diffusion coefficients cannot be matched, one should refer to Appendix S.I for calibration. Finally, if concentrations cannot be matched, one should resort to digital simulations.

ACKNOWLEDGMENT

We gratefully acknowledge support from the Petroleum Research Fund, administered by the American Chemical Soxiety (Grant 35154-AC5).

SUPPORTING INFORMATION AVAILABLE

Appendix S.I, computer-generated data for the $(i_{l,R_2}/i_{l,R_1})_N$ ratio as a function of D_{R_1}/D_{R_2} and D_{R_2}/D_{O_2}. Appendixes S.II and S.III, overlapping simulated voltammograms of the dMeFc/Fc and of the $[Co(bipy)_3]^{2+}$/MePTZ system, respectively, in the absence and presence of eq 4. This material is available free of charge via the Internet at http://pubs.acs.org

Received for review May 2, 2003. Accepted July 10, 2003.

AC030176U